Dissecting Soft Radiation with Factorization

Iain W. Stewart, Frank J. Tackmann, and Wouter J. Waalewijn

Dissecting Soft Radiation with Factorization

Iain W. Stewart,[1] Frank J. Tackmann,[2] and Wouter J. Waalewijn[3, 4]

[1] *Center for Theoretical Physics, Massachusetts Institute of Technology, Cambridge, MA 02139, USA*
[2] *Theory Group, Deutsches Elektronen-Synchrotron (DESY), D-22607 Hamburg, Germany*
[3] *Nikhef, Theory Group, Science Park 105, 1098 XG, Amsterdam, The Netherlands*
[4] *ITFA, University of Amsterdam, Science Park 904, 1018 XE, Amsterdam, The Netherlands*

An essential part of high-energy hadronic collisions is the soft hadronic activity that underlies the primary hard interaction. It includes soft radiation from the primary hard partons, secondary multiple parton interactions (MPI), and factorization violating effects. The invariant mass spectrum of the leading jet in Z+jet and H+jet events is directly sensitive to these effects, and we use a QCD factorization theorem to predict its dependence on the jet radius R, jet p_T, jet rapidity, and partonic process for both the perturbative and nonperturbative components of primary soft radiation. We prove that the nonperturbative contributions involve only odd powers of R, and the linear R term is universal for quark and gluon jets. The hadronization model in PYTHIA8 agrees well with these properties. The perturbative soft initial state radiation (ISR) has a contribution that depends on the jet area in the same way as the underlying event, but this degeneracy is broken by dependence on the jet p_T. The size of this soft ISR contribution is proportional to the color state of the intial partons, yielding the same positive contribution for $gg \to Hg$ and $gq \to Zq$, but a negative interference contribution for $q\bar{q} \to Zg$. Hence, measuring these dependencies allows one to separate hadronization, soft ISR, and MPI contributions in the data.

Soft hadronic activity plays a role in practically all but the most inclusive measurements at the LHC. It is often an important yet hard-to-quantify source of uncertainty, so improving its theoretical understanding is vital. One can consider four conceptually different sources for the effects that are experimentally associated with soft hadronic activity and the underlying event (UE):

1. Perturbative soft radiation from the primary incoming and outgoing hard partons within factorization

2. Nonperturbative soft effects within factorization associated with hadronization

3. Multiple parton interactions (MPI) at lower scales in the same proton-proton collision

4. Factorization breaking contributions

For any given observable, the question is how much of each of these sources is required to describe the data. For example, it is known that including higher-order perturbative corrections (source 1) in parton-shower Monte Carlo programs can give a nontrivial contribution to traditional UE measurements [1, 2].

Traditionally, the UE activity is measured in regions of phase space away from hard jets [2–12]. These results are used to tune the MPI models which describe the UE in Monte Carlo programs [13–18]. These models are then extrapolated into the jet region, where they are used to describe various jet observables, including the jet mass spectrum in dijet and Drell-Yan events [19, 20], which is an important benchmark jet observable at the LHC.

In this paper, we directly consider the jet region and give a field-theoretic description of primary soft effects (sources 1 and 2), and discuss how to distinguish sources 1, 2, and 3. This is done using the dependence of the jet mass spectrum and its first moment on the jet radius R, jet momentum p_T^J, jet rapidity y_J, and participating partons. We will not consider factorization breaking effects here (see e.g. Ref. [21]).

We consider the jet mass spectrum in exclusive $pp \to Z$+1-jet and $pp \to H$+1-jet events. The factorization formula for $m_J \ll p_T^J$ that includes sources 1 and 2 is given by [22–24]

$$\frac{\mathrm{d}\sigma}{\mathrm{d}m_J^2 \mathrm{d}\Phi_2} = \sum_{\kappa,a,b} H_\kappa(\Phi_2) \int \mathrm{d}k_S \mathrm{d}k_B \left(\mathcal{I}_{\kappa_a a} \mathcal{I}_{\kappa_b b} \otimes f_a f_b\right)(k_B)$$
$$\times J_{\kappa_J}(m_J^2 - 2p_T^J k_S)\, S_\kappa(k_S, p^{\mathrm{cut}} - k_B, y_J, R)\,. \qquad (1)$$

Here, $\Phi_2 = \{p_T^J, y_J, Y\}$, Y is the rapidity of the Z/H+jet system, κ denotes the partonic channel, and k_S and k_B enable soft contributions to the jet mass m_J^2 and jet veto p^{cut} (which vetoes additional jets). The $H_\kappa(\Phi_2)$ contains the perturbative matrix elements for the hard process, and $\mathcal{I}_{\kappa_a a} \mathcal{I}_{\kappa_b b} \otimes f_a f_b$ describes perturbative collinear initial-state radiation convolved with the parton distribution functions. For the normalized jet mass spectrum, the dependence on p^{cut} largely drops out [24]. As a result, the shape of the jet mass spectrum is determined by the jet function J_{κ_J}, describing energetic final-state radiation, and by the soft function S_κ. See also Refs. [25, 26].

The soft function S_κ describes the primary initial and final state soft radiation. It depends on the jet through y_J and R but not p_T^J, and can be factorized as [27–29]

$$S_\kappa(k_S, k_B, y_J, R) = \int \mathrm{d}k\, S_\kappa^{\mathrm{pert}}(k_S - k, k_B, y_J, R) \qquad (2)$$
$$\times F_\kappa(k, y_J, R)\left[1 + \mathcal{O}\left(\Lambda_{\mathrm{QCD}}/k_B\right)\right],$$
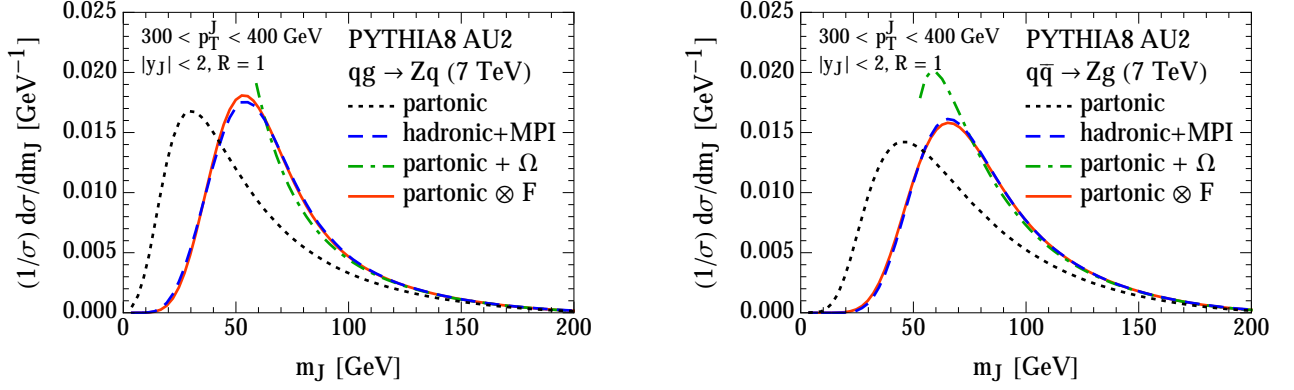
FIG. 1. For the jet mass spectrum in PYTHIA8, the change from partonic to hadronization+MPI is described by a simple shift in the tail, and a simple convolution everywhere, for both quark jets (left panel) and gluon jets (right panel).

where S_κ^{pert} contains the perturbative soft contributions. F_κ is a normalized nonperturbative shape function which encodes the smearing effect that the hadronization has on the soft momentum k_S. For $k_S \sim \Lambda_{\text{QCD}}$, the full $F_\kappa(k)$ is required and shifts the peak region of the jet mass spectrum to higher jet masses.

In the perturbative tail of the jet mass spectrum, where $k_S \gg \Lambda_{\text{QCD}}$, S_κ can be expanded,

$$S_\kappa(k_S, y_J, R) = S_\kappa^{\text{pert}}\big(k_S - \Omega_\kappa(R), y_J, R\big) \\ + \mathcal{O}\big(\Lambda_{\text{QCD}}^2/k_S^3, \alpha_s \Lambda_{\text{QCD}}/k_S^2\big), \quad (3)$$

where $\Omega_\kappa(R) = \int dk\, k\, F_\kappa(k) \sim \Lambda_{\text{QCD}}$ is a nonperturbative parameter. In this region factorization predicts a shift in the jet mass spectrum, which is described by $\Omega_\kappa(R)$. Below, we use the field-theoretic definition of Ω_κ to quantify its R-dependence and prove that it is independent of y_J. The above treatment provides an excellent description of hadronization in both B-meson decays and e^+e^- event shapes [30, 31].

Factorization also underlies the Monte Carlo description of the primary collision, where H corresponds to the hard matrix element, while $\mathcal{I}$, J, and S are described by parton showers, and F corresponds to the hadronization models. The standard parton shower paradigm does not completely capture interference effects between wide-angle soft emissions from different primary partons that appear at $\mathcal{O}(\alpha_s)$ in S_κ. Monte Carlo programs include MPI (source 3), which are not in Eq. (1). See Ref. [32] for a recent discussion. For our numerical studies, we consider both PYTHIA8 [33, 34] with the ATLAS underlying event tune AU2-MSTW2008LO [16] and HERWIG++ 2.7 [35, 36] with its default underlying event tune UE-EE-5-MRST [18]. Both give a reasonable description of the CMS jet mass spectrum in Z+jet events [20]. We also compare to the PYTHIA8 default tune 4C.

We consider exclusive Z/H+jet events at $E_{\text{cm}} = 7$ TeV in both quark and gluon channels, with the leading jet within a certain range of p_T^J and y_J, and we veto additional jets with $p_T^J > 50$ GeV. The jets are defined using

anti-k_T [37, 38]. In Fig. 1, we show the jet mass spectrum for quark and gluon jets with $R = 1$ after parton showering (black dotted) and including both hadronization and MPI (blue dashed). Eq. (3) predicts that for $m_J^2 \gg \Lambda_{\text{QCD}} p_T^J$ the nonperturbative corrections shift the tail of the jet mass spectrum by

$$m_J^2 = (m_J^2)^{\text{pert}} + 2p_T^J\, \Omega_\kappa(R). \quad (4)$$

We can regard the partonic result from PYTHIA8 as the baseline purely perturbative result. Choosing $\Omega = 2.4$ GeV for $qg \to Zq$ and $\Omega = 2.7$ GeV for $q\bar{q} \to Zg$ yields the green dot-dashed curves in Fig. 1. We see that the effect of both hadronization and MPI in the tail is well captured by this shift. For hadronization, Eqs. (1,2) predict a convolution with a nonperturbative function,

$$\frac{d\sigma_\kappa}{dm_J^2} = \int dk\, \frac{d\sigma_\kappa^{\text{partonic}}}{dm_J^2}(m_J^2 - 2p_T^J k)\, F_\kappa(k). \quad (5)$$

With the above Ωs, this convolution gives the red solid curves in Fig. 1, yielding excellent agreement with the hadronization+MPI result over the full range of the jet mass spectrum.[1] Both hadronization and MPI populate the jet region with a smooth background of soft particles, which can explain why the MPI effect is reproduced alongside the hadronization by a convolution of the form Eq. (5). This apparent degeneracy motivates us to determine the calculable behavior of the jet mass spectrum due to primary perturbative and nonperturbative soft radiation within factorization, study its dependence on p_T^J, y_J, and R, and compare these results to Monte Carlo program contributions for soft ISR, hadronization, and MPI.

––––––––

[1] Here, $F_\kappa(k) = (4k/\Omega_\kappa^2)\, e^{-2k/\Omega_\kappa}$; the simplest ansatz that satisfies the required properties: normalization, vanishing at $k = 0$, falling off exponentially for $k \to \infty$, and having a first moment Ω_κ. Fixing the value of Ω_κ from the tail, we find similar levels of agreement across all values of p_T^J, y_J, R, for all partonic channels, and for different jet veto cuts (including no jet veto).
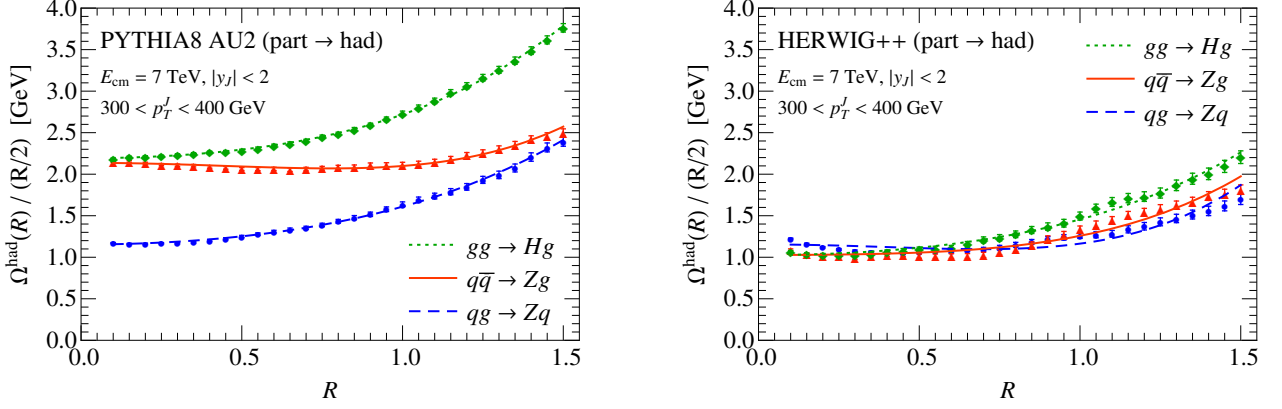
FIG. 2. The R dependence of $\Omega_\kappa^{\mathrm{had}}(R)$ extracted from M_1 in PYTHIA8 (left panel) and HERWIG++ (right panel), shown as dots, triangles and squares for different channels. The fit using Eq. (9) (shown by lines) demonstrates the agreement with factorization. The small-R behavior only depends on whether the jet is initiated by a quark (blue dashed) or gluon (orange solid and green dotted).

We consider the first moment in m_J^2,

$$M_1 = \frac{1}{\sigma} \int dm_J^2 \, m_J^2 \, \frac{d\sigma}{dm_J^2} \,, \tag{6}$$

which tracks the shift observed in Fig. 1. Taking the first moment of Eq. (1) combined with Eqs. (2) and (3), we can compute the dependence of primary soft radiation on p_T^J, y_J, R, and partonic channel, giving

$$M_1 = M_{1\,\kappa}^{\mathrm{pert}}(p_T^J, y_J, R) + 2p_T^J \, \Omega_\kappa(R) \,. \tag{7}$$

Here, $M_{1\,\kappa}^{\mathrm{pert}}(p_T^J, y_J, R)$ contains all perturbative contributions, while $\Omega_\kappa(R)$ encodes the shift due to nonperturbative effects.

For $pp \to H/Z$+jet, $\Omega_\kappa(R)$ is given by the vacuum matrix element of lightlike soft Wilson lines Y_a, Y_b, and $Y_J \equiv Y_J(y_J, \phi_J)$ along the beam and jet directions,

$$\Omega_\kappa(R) = \int_0^1 dr \int_{-\infty}^{\infty} dy \int_0^{2\pi} d\phi \, f(r, y - y_J, \phi - \phi_J, R)$$
$$\times \langle 0 | \bar{T}[Y_J^\dagger Y_b^\dagger Y_a^\dagger] \, \hat{\mathcal{E}}_T(r, y, \phi) T[Y_a Y_b Y_J] | 0 \rangle \,. \tag{8}$$

Here, the rapidity y, azimuthal angle ϕ, and transverse velocity $r = p_T/m_T$ are measured with respect to the beam axis. The color representation of the Wilson lines depends on the partonic channel, giving the κ dependence of Ω_κ. The jet mass measurement function is $f(r, y, \phi, R) = (\cosh y - r \cos \phi) \, \theta[b(y, \phi, r) < R^2]$ where $b(y, \phi, r)$ specifies the jet boundary. The matrix element involves the energy flow operator [39–43] $\hat{\mathcal{E}}_T(r, y, \phi)|X\rangle = \sum_{i \in X} m_{Ti} \delta(r - r_i) \delta(y - y_i) \delta(\phi - \phi_i)|X\rangle$. From Eq. (8) it follows immediately that $\Omega_\kappa(R)$ is independent of p_T^J. Using invariance under boosts and rotations, we can prove that it is also independent of y_J and ϕ_J [44].

Expanding Eq. (8) for small R, we find [44, 45]

$$\Omega_\kappa(R) = \frac{R}{2} \Omega_\kappa^{(1)} + \frac{R^3}{8} \Omega_\kappa^{(3)} + \frac{R^5}{32} \Omega_\kappa^{(5)} + \mathcal{O}\left[\left(\frac{R}{2}\right)^7\right], \tag{9}$$

where the $\Omega_\kappa^{(i)}$ are R independent and only odd powers of R occur. This R-scaling of our nonperturbative operator for jet mass agrees with that found in Ref. [46] from a QCD hadronization model. Our operator definition implies a universality for the linear R nonperturbative parameter in Eq. (9). For $R \to 0$ the beam Wilson lines fuse into a Wilson line in the conjugate representation to the jet, $Y_a Y_b \to Y_{\bar{J}}$. The result is given by [44]

$$\Omega_\kappa^{(1)} = \int_0^1 dr' \langle 0 | \bar{T}[Y_J^\dagger Y_{\bar{J}}^\dagger] \hat{\mathcal{E}}_\perp(r') T[Y_{\bar{J}} Y_J] | 0 \rangle \,, \tag{10}$$

which only depends on whether the jet is a quark or gluon jet. For quarks, we can compare this to thrust in DIS [47] where precisely this parameter $\Omega_q^{(1)}$ appears [48].

Consider next $M_{1\,\kappa}^{\mathrm{pert}}$ in Eq. (7). Dimensional analysis and the kinematical bound $m_J \lesssim p_T^J R$ imply that $M_{1\,\kappa}^{\mathrm{pert}}$ scales like $(p_T^J R)^2$. Resummation modifies the leading R dependence to $R^{2-\gamma_\kappa}$, where $\gamma_\kappa \sim \alpha_s > 0$. The soft function contains a contribution due to interference between ISR from the two beams [44],

$$S_\kappa^{\mathrm{pert}}(k_S) \supset \frac{\alpha_s C_\kappa}{\pi} R^2 \frac{1}{\mu} \left(\frac{\mu}{k_S}\right)_+ \,. \tag{11}$$

This soft ISR contributes to $M_{1\,\kappa}^{\mathrm{pert}}$ as $(p_T^J)^2 R^4$ with the color factors

$$C_{qg \to q} = C_{gg \to g} = \frac{C_A}{2} = \frac{3}{2} \,,$$
$$C_{q\bar{q} \to g} = C_F - \frac{C_A}{2} = -\frac{1}{6} \,. \tag{12}$$

The above factorization results can be compared to PYTHIA8 and HERWIG++, where we find that the dependence of M_1 on p_T^J, y_J, κ, is well described by

$$M_1 = M_{1\,\kappa}^{\mathrm{partonic}}(p_T^J, y_J, R) + 2p_T^J \, \Omega_\kappa^{\mathrm{had}}(R)$$
$$+ 2p_T^J \left[\Upsilon^{\mathrm{MPI}}(y_J, R) + \Omega_\kappa^{\mathrm{MPI}}(y_J, R)\right]. \tag{13}$$
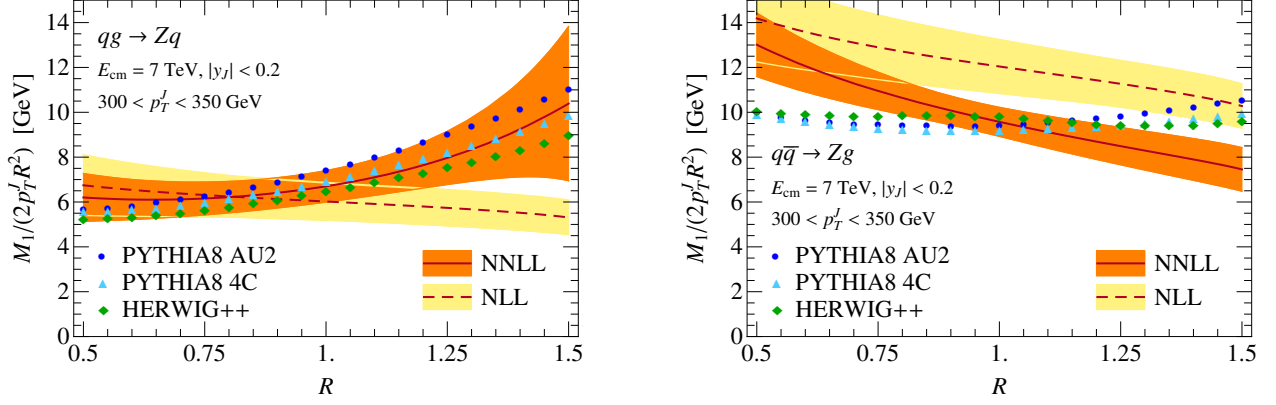
FIG. 3. R dependence of the perturbative jet mass moment $M_{1\,\kappa}^{\text{pert}}$ at NLL and NNLL and the partonic jet mass moment $M_{1\,\kappa}^{\text{partonic}}$ in PYTHIA8 (tune AU2 and 4C) and HERWIG++ for $qg \to Zq$ (left panel) and $q\bar{q} \to Zg$ (right panel). The soft ISR contribution $\sim R^4$ is well modelled by Monte Carlo programs for $qg \to Zq$, but not for the destructive interference in $q\bar{q} \to Zg$.
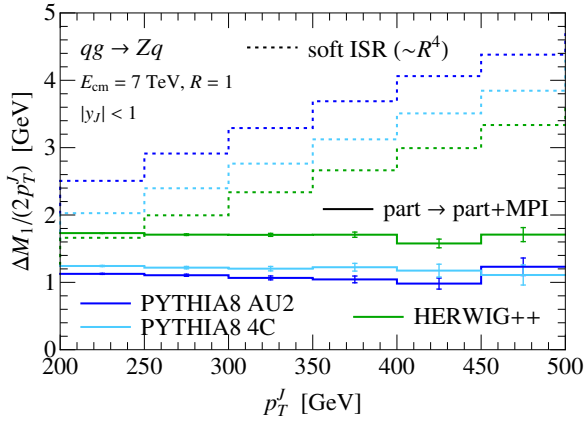

FIG. 4. p_T^J dependence of the $\sim R^4$ contributions to the jet mass moment in PYTHIA8 and HERWIG++ from MPI (solid lines from Υ^{MPI}), and soft ISR (dashed lines from c_4^κ in Eq. (14)) for $qg \to Zq$. They can be distinguished by their p_T^J dependence.

Here, $M_{1\,\kappa}^{\text{partonic}}$ is the partonic contribution, $\Omega_\kappa^{\text{had}}$ is defined by partonic $\to$ hadronic, and Υ^{MPI} by partonic $\to$ partonic+MPI. The small remainder from hadronization of the MPI, $\Omega_\kappa^{\text{MPI}}$, is defined to ensure the sum of terms yields the full partonic $\to$ hadronic+MPI. Note that hadronization and MPI contributions are each individually described by shifts to M_1. Also, the independence of Ω_κ to y_J and ϕ_J is observed in both PYTHIA8 and HERWIG++ [44]. Eq. (13) contains MPI contributions with no analog in Eq. (7).

The hadronization $\Omega_\kappa^{\text{had}}(R)/(R/2)$ from PYTHIA8 and HERWIG++ is shown in Fig. 2 for different channels. For $R \ll 1$, $\Omega_\kappa^{\text{had}}(R)$ is linear in R and has the same slope for the two channels involving gluon jets, as predicted by factorization. For PYTHIA8, all channels differ for large R and can be fit to the factorization form in Eq. (9). For the quark jet we extract $\Omega_q^{(1)} = 1.2\,\text{GeV}$ and for gluon jets $\Omega_g^{(1)} = 2.2\,\text{GeV}$. For $qg \to Zq$ and $gg \to Hg$ the

R dependence is strong enough that an additional R^2 contribution is disfavored in the fit. For HERWIG++, the dependence on higher powers of R is much weaker, and $\Omega_g^{(1)} \approx \Omega_q^{(1)}$. The full set of fit coefficients are in [44].

In Fig. 3, we compare our perturbative NLL and NNLL factorization predictions [24] for $M_{1\,\kappa}^{\text{pert}}$ to the corresponding $M_{1\,\kappa}^{\text{partonic}}$ from PYTHIA8 and HERWIG++ as a function of R, dividing by the leading R^2 dependence. The R^4 contribution from soft ISR only enters at NNLL and is seen in the rise at large R for $qg \to Zq$ (left panel). This effect is partially modeled by soft emissions in the parton shower, which explains the similar R^4 contribution for $qg \to Zq$ in PYTHIA8 and HERWIG++. For $q\bar{q} \to Zg$ (right panel) Eqs. (11) and (12) predict the R^4 contribution from soft ISR to be negative, which we observe at NNLL. This negative interference effect is not captured by these Monte Carlo programs.

The apparent ambiguity between R^4 contributions from soft ISR and MPI can be resolved through their p_T^J dependence. In Fig. 4, we show the R^4 component, c_4^κ, of the partonic moment, obtained by fitting

$$\frac{M_{1\,\kappa}^{\text{part}}}{2p_T^J R^2} = c_2^\kappa R^{-\gamma_\kappa} + c_4^\kappa R^2 , \qquad (14)$$

and also the MPI contribution to the moment, $\Upsilon^{\text{MPI}}/R^2 \sim R^2$. The differences between various tunes for c_4^κ and Υ^{MPI} reflects their apparent ambiguity, whereas their sum agree much better. The p_T^J dependence clearly resolves the ambiguity: $c_4^\kappa \sim p_T^J$ as predicted by factorization, whereas Υ^{MPI} is independent of p_T^J. As shown in Ref. [44]: the channel dependence could also be used to separate soft ISR from MPI: c_4^κ depends on the color channel as in Eq. (12), whereas Υ^{MPI} is channel independent. Also, the y_J dependence of soft ISR is quite different between HERWIG++ and PYTHIA8.

To conclude, we have used QCD factorization to predict the properties of the perturbative and nonperturbative components of primary soft radiation for jet mass

in $pp \rightarrow H/Z+$jet. We have shown that the nonperturbative soft effects involve odd powers of R and are universal for quark and gluon jets for $R \ll 1$. Hadronization models in Monte Carlo programs agree with these predictions. The perturbative soft radiation has a contribution that scales like R^4, just like the contribution from MPI. These components depend differently on p_T^J and on the partonic process. Hence, separately measuring quark and gluon channels in Drell-Yan and in different bins of p_T^J provides the possibility to clearly distinguish between MPI and primary soft radiation.

[1] M. Cacciari, G. P. Salam, and S. Sapeta, JHEP **1004**, 065 (2010), arXiv:0912.4926 [hep-ph].

[2] S. Chatrchyan et al. (CMS Collaboration), Eur. Phys. J. C **72**, 2080 (2012), arXiv:1204.1411 [hep-ex].

[3] T. Affolder et al. (CDF Collaboration), Phys. Rev. D **65**, 092002 (2002).

[4] D. Acosta et al. (CDF Collaboration), Phys. Rev. D **70**, 072002 (2004), hep-ex/0404004.

[5] R. Field and R. C. Group (CDF Collaboration), (2005), hep-ph/0510198.

[6] T. Aaltonen et al. (CDF Collaboration), Phys. Rev. D **82**, 034001 (2010), arXiv:1003.3146 [hep-ex].

[7] R. Field, (2010), arXiv:1010.3558 [hep-ph].

[8] G. Aad et al. (ATLAS Collaboration), (2010), ATL-PHYS-PUB-2010-014.

[9] G. Aad et al. (ATLAS Collaboration), Phys. Rev. D **83**, 112001 (2011), arXiv:1012.0791 [hep-ex].

[10] G. Aad et al. (ATLAS Collaboration), (2011), ATL-PHYS-PUB-2011-009.

[11] G. Aad et al. (ATLAS Collaboration), Eur. Phys. J. C **71**, 1636 (2011), arXiv:1103.1816 [hep-ex].

[12] S. Chatrchyan et al. (CMS Collaboration), JHEP **1109**, 109 (2011), arXiv:1107.0330 [hep-ex].

[13] A. Buckley, H. Hoeth, H. Lacker, H. Schulz, and J. E. von Seggern, Eur. Phys. J. C **65**, 331 (2010), arXiv:0907.2973 [hep-ph].

[14] P. Z. Skands, Phys. Rev. D **82**, 074018 (2010), arXiv:1005.3457 [hep-ph].

[15] A. Buckley, J. Butterworth, S. Gieseke, D. Grellscheid, S. Hoche, et al., Phys. Rept. **504**, 145 (2011), arXiv:1101.2599 [hep-ph].

[16] G. Aad et al. (ATLAS Collaboration), (2012), ATL-PHYS-PUB-2012-003.

[17] S. Gieseke, C. Rohr, and A. Siodmok, Eur. Phys. J. C **72**, 2225 (2012), arXiv:1206.0041 [hep-ph].

[18] M. H. Seymour and A. Siodmok, JHEP **1310**, 113 (2013), arXiv:1307.5015 [hep-ph].

[19] G. Aad et al. (ATLAS), JHEP **1205**, 128 (2012), arXiv:1203.4606 [hep-ex].

[20] S. Chatrchyan et al. (CMS Collaboration), JHEP **1305**, 090 (2013), arXiv:1303.4811 [hep-ex].

[21] J. R. Forshaw, M. H. Seymour, and A. Siodmok, JHEP **1211**, 066 (2012), arXiv:1206.6363 [hep-ph].

[22] I. W. Stewart, F. J. Tackmann, and W. J. Waalewijn, Phys. Rev. Lett. **105**, 092002 (2010), arXiv:1004.2489 [hep-ph].

[23] T. T. Jouttenus, I. W. Stewart, F. J. Tackmann, and W. J. Waalewijn, Phys. Rev. D **83**, 114030 (2011), arXiv:1102.4344 [hep-ph].

[24] T. T. Jouttenus, I. W. Stewart, F. J. Tackmann, and W. J. Waalewijn, Phys. Rev. D **88**, 054031 (2013), arXiv:1302.0846 [hep-ph].

[25] M. Dasgupta, K. Khelifa-Kerfa, S. Marzani, and M. Spannowsky, JHEP **1210**, 126 (2012), arXiv:1207.1640 [hep-ph].

[26] Y.-T. Chien, R. Kelley, M. D. Schwartz, and H. X. Zhu, Phys. Rev. D **87**, 014010 (2013), arXiv:1208.0010 [hep-ph].

[27] G. P. Korchemsky and G. Sterman, Nucl. Phys. B **555**, 335 (1999), hep-ph/9902341.

[28] A. H. Hoang and I. W. Stewart, Phys. Lett. B **660**, 483 (2008), arXiv:0709.3519 [hep-ph].

[29] Z. Ligeti, I. W. Stewart, and F. J. Tackmann, Phys. Rev. D **78**, 114014 (2008), arXiv:0807.1926 [hep-ph].

[30] F. U. Bernlochner et al. (SIMBA), PoS **ICHEP2012**, 370 (2013), arXiv:1303.0958 [hep-ph].

[31] R. Abbate, M. Fickinger, A. H. Hoang, V. Mateu, and I. W. Stewart, Phys. Rev. D **83**, 074021 (2011), arXiv:1006.3080 [hep-ph].

[32] J. R. Gaunt, (2014), arXiv:1405.2080 [hep-ph].

[33] T. Sjöstrand, S. Mrenna, and P. Skands, JHEP **05**, 026 (2006), hep-ph/0603175.

[34] T. Sjöstrand, S. Mrenna, and P. Skands, Comput. Phys. Commun. **178**, 852 (2008), arXiv:0710.3820 [hep-ph].

[35] M. Bahr, S. Gieseke, M. Gigg, D. Grellscheid, K. Hamilton, et al., Eur. Phys. J. C **58**, 639 (2008), arXiv:0803.0883 [hep-ph].

[36] J. Bellm, S. Gieseke, D. Grellscheid, A. Papaefstathiou, S. Platzer, et al., (2013), arXiv:1310.6877 [hep-ph].

[37] M. Cacciari, G. P. Salam, and G. Soyez, JHEP **04**, 063 (2008), arXiv:0802.1189 [hep-ph].

[38] M. Cacciari, G. P. Salam, and G. Soyez, Eur. Phys. J. C **72**, 1896 (2012), arXiv:1111.6097 [hep-ph].

[39] N. A. Sveshnikov and F. V. Tkachov, Phys. Lett. B **382**, 403 (1996), hep-ph/9512370.

[40] P. Cherzor and N. Sveshnikov, Proceedings of the QFTHEP'97 Workshop, arXiv:hep-ph/9710349.

[41] A. V. Belitsky, G. P. Korchemsky, and G. Sterman, Phys. Lett. **B515**, 297 (2001), arXiv:hep-ph/0106308.

[42] C. Lee and G. F. Sterman, Phys. Rev. D **75**, 014022 (2007), hep-ph/0611061.

[43] V. Mateu, I. W. Stewart, and J. Thaler, Phys. Rev. **D87**, 014025 (2013), arXiv:1209.3781 [hep-ph].

[44] See Supplemental Material for additional details.

[45] C. Marcantonini and I. W. Stewart, Phys. Rev. **D79**, 065028 (2009), arXiv:0809.1093 [hep-ph].

[46] M. Dasgupta, L. Magnea, and G. P. Salam, JHEP **02**, 055 (2008), arXiv:0712.3014 [hep-ph].

[47] M. Dasgupta and G. P. Salam, JHEP **0208**, 032 (2002), hep-ph/0208073 [hep-ph].

[48] D. Kang, C. Lee, and I. W. Stewart, Phys. Rev. D **88**, 054004 (2013), arXiv:1303.6952 [hep-ph].